A structural and magnetic study of the defect perovskite $LaNiO_{2.5}$ from high-resolution neutron diffraction data

1997 J. Phys.: Condens. Matter 9 6417

(http://iopscience.iop.org/0953-8984/9/30/010)

J. Phys.: Condens. Matter **9** (1997) 6417–6426. Printed in the UK PII: S0953-8984(97)83004-4

A structural and magnetic study of the defect perovskite $LaNiO_{2.5}$ from high-resolution neutron diffraction data

J A Alonso†, M J Martínez-Lope†, J L García-Muñoz‡ and M T Fernández-Díaz§

† Instituto de Ciencia de Materiales de Madrid, CSIC, Cantoblanco, E-28049 Madrid, Spain
‡ Instituto de Ciencia de Materiales de Barcelona, CSIC, Bellaterra, E-28193 Barcelona, Spain
§ Institut Laue–Langevin, BP 156X, 38042 Grenoble Cédex 9, France

Received 26 March 1997

Abstract. The fine details of the crystal structure of $LaNiO_{2.5}$ have been determined from a high-resolution neutron diffraction study at room temperature. The powder sample, showing an excellent crystallinity, was prepared by topotactic reduction of $LaNiO_3$ in the presence of Zr. The unit cell can be described as a monoclinic $2a_0 \times 2a_0 \times 2a_0$ superstructure of perovskite (a_0 is the edge of the ideal perovskite), and contains one-dimensionally infinite chains of flattened NiO_6 octahedra running parallel to the $\boldsymbol{c}$ axis, with NiO_4 square planar units connecting the octahedra chains. Bond valence calculations are consistent with divalent Ni cations in both coordination polyhedra. Neutron diffraction experiments reveal 3D magnetic ordering below $T_N \approx 80$ K. A magnetic structure with $S = 1$ moments antiferromagnetically coupled along the NiO_6 chains parallel to the $\boldsymbol{c}$ axis is proposed, and the absence of magnetic moments at the NiO_4 units is also discussed.

1. Introduction

Recently the perovskites $RNiO_3$ (R = rare earth) have attracted considerable attention since they are among the few transition metal oxides that exhibit metallic properties or metal-to-insulator (MI) transitions [1]. In this family of oxides the transition temperature T_{MI} rises systematically as the rare-earth size becomes smaller, i.e., as the distortion of the perovskite with respect to the ideal structure (aristotype) increases [2]. For $LaNiO_3$ the large size of La determines a slightly distorted rhombohedral structure (space group $R\bar{3}c$), which, in fact, keeps its metallic character down to 1.5 K, showing no MI transition [3]. $RNiO_3$ oxides (R = Pr, Nd, Sm, Eu) are orthorhombic, crystallize in the $GdFeO_3$ structure (space group $Pbnm$) and exhibit MI transitions at 130 K (Pr), 200 K (Nd), 400 K (Sm) and 460 K (Eu) [2].

Reliable structural information about some of these perovskites has been obtained by neutron powder diffraction for R = La, Pr, Nd [4]. The precise knowledge of the crystal structure of these phases has shown to be of paramount importance in the interpretation of the MI transitions, the temperature of which can be correlated to the Ni–O–Ni angles, governing the transfer integral between Ni 3d and O 2p orbitals.

In this family of perovskite oxides, nickel cations adopt a trivalent oxidation state. Small changes in the Ni valence can result in dramatic changes in the transport and magnetic properties of these materials, as recently shown in a series of doped phases of composition $R_{1-x}A_xNiO_3$ [5, 6], in which holes or electrons are injected by appropriate cationic substitution at the rare-earth positions of the perovskite structure.

0953-8984/97/306417+10$19.50

The Ni oxidation state can also be controlled by the oxygen content of the material. Topotactic deintercalation of oxide ions has been shown to be possible in this family of perovskites since the pioneering work by Gai and Rao [7], who reported the existence of a homologous series of composition $La_nNi_nO_{3n-1}$ on the basis of a thermogravimetric study of $LaNiO_3$ in air. The $n = 1, 2$ members of this series, $LaNiO_2$ and $LaNiO_{2.5}$ (or $La_2Ni_2O_5$), were subsequently isolated by Crespin and co-workers [8, 9] by low-temperature reduction of $LaNiO_3$ under hydrogen.

The crystal structure and physical properties of the defect perovskite $LaNiO_{2.5}$, with an average oxidation state for Ni of 2+, have been controversial for a long time. The x-ray powder diffraction (XRD) pattern was first reported by Crespin *et al* [8] and indexed on the basis of a superstructure of perovskite in which the relationship to the aristotype (or ideal perovskite cubic unit cell with $a = a_0 \approx 4$ Å) was $2\sqrt{2}a_0 \times 2\sqrt{2}a_0 \times 2a_0$. Later on, Vidyasagar *et al* [10] and Rao *et al* [11] postulated a tetragonal cell ($a = 7.816$ Å, $c = 7.468$ Å) for $LaNiO_{2.5}$, and proposed a structural model involving the ordering of the oxygen vacancies along the [1 1 0] direction in the [0 0 1] planes of the lattice, giving rise to square planar and octahedral coordinations for Ni^{2+}, according to the site energy preference of Ni^{2+} for square planar rather than tetrahedral coordination. The true cell dimensions were finally reported by Moriga *et al* [12, 13], who found from XRD data a monoclinic superstructure of perovskite $2a_0 \times 2a_0 \times 2a_0$ and gave a tentative description of the structure.

Recently, a medium-resolution neutron powder diffraction (NPD) study of a good-quality $LaNiO_{2.5}$ polycrystalline sample prepared by an original method, based on the reduction of $LaNiO_3$ with Zr as oxygen getter, allowed us to determine the tilting scheme of the Ni coordination polyhedra [14]. On the basis of this model, the structure has now been refined by the Rietveld method from high-resolution NPD data. This paper aims to describe the fine-structural features of the defect $LaNiO_{2.5}$ perovskite as well as to discuss the implications of a bond valence study on the Ni oxidation state in the oxygen coordination polyhedra of Ni cations. Moreover, we have broached the study of its low-temperature magnetic behaviour by NPD: a consistent picture emerges from both structural and magnetic data.

2. Experimental details

A black polycrystalline sample of $LaNiO_{2.5}$ was prepared by topotactic reduction of $LaNiO_3$ in the presence of Zr. Details on the preparation of the precursor perovskite $LaNiO_3$ and the reduction procedure are given elsewhere [14]. The product was characterized by XRD using Cu Kα radiation, in a Siemens D-501 goniometer controlled by a DACO-MP computer, by step-scanning from 10 to 100° in 2θ, in increments of 0.05° and a counting time of 4 s each step.

NPD data of $LaNiO_{2.5}$ were collected at room temperature in the high-resolution D2B diffractometer at ILL, Grenoble, by step-scanning between 0 and 162° 2θ with increments of 0.05°. A wavelength of 1.594 Å was selected from a Ge monochromator. About 10 g sample was contained in a cylindrical vanadium can. The total counting time was approximately 3 h. The thermal evolution of the sample was studied down to 1.5 K in the G41 multidetector diffractometer, at the Orphée reactor of the CEN-Saclay, with a wavelength of 2.426 Å selected from a graphite monochromator. The position sensitive detector, with 800 cells covering a 2θ range of 80°, was kept in a fixed position during all the data collection for each experiment. The diffraction patterns were collected, by heating, every 10 K in 15 min.

All the diffraction patterns were analysed by the Rietveld method, using the FULLPROF refinement program [15]. A pseudo-Voigt function was chosen to generate the line shape of

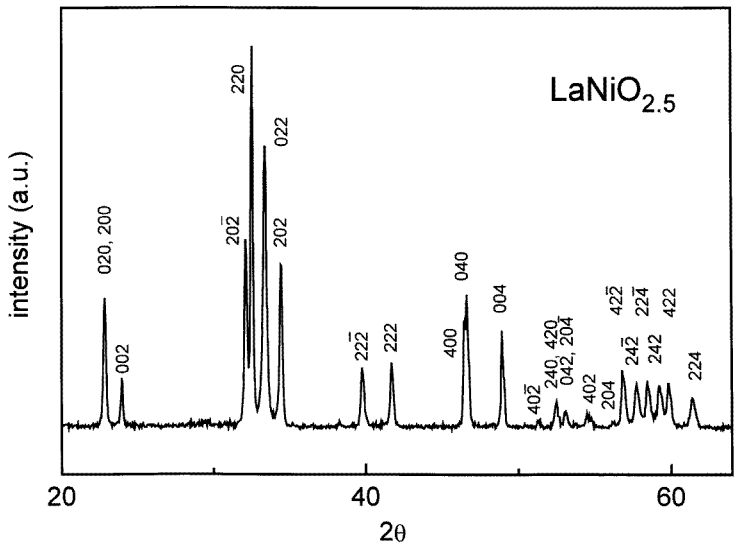

Figure 1. An XRD diagram of $LaNiO_{2.5}$. The peaks are indexed according to a doubled monoclinic unit cell with dimensions $a = 7.8413(7)$ Å, $b = 7.7947(7)$ Å, $c = 7.4668(6)$ Å and $\beta = 93.875(5)^\circ$.

the diffraction peaks. The coherent scattering lengths for La, Ni and O were, respectively, 8.24, 10.3 and 5.805 fm. For the high-resolution data the following parameters were refined in the final run: six background coefficients, zero point, half-width, pseudo-Voigt and asymmetry parameters for the peak shape, scale factor, atomic positions, thermal isotropic factors and unit-cell parameters. For the neutron data collected at the G41 diffractometer in a more restricted angular range, with lower resolution at high angles, the atomic coordinates were fixed to those determined for the high-resolution room-temperature data, and an overall thermal B factor was refined together with the unit-cell parameters and the magnitude of the moments of the magnetic structure.

3. Results

3.1. Room-temperature structural refinement

Figure 1 shows the XRD pattern of the defect perovskite $LaNiO_{2.5}$, showing a sharp monoclinic splitting of the diffraction peaks. The XRD reflections are indexed in a monoclinic unit cell with dimensions $a = 7.8413(7)$ Å, $b = 7.7947(7)$ Å, $c = 7.4668(6)$ Å and $\beta = 93.875(5)^\circ$, corresponding to a $2a_0 \times 2a_0 \times 2a_0$ superstructure of perovskite. Note that the Miller indices of all the peaks in figure 1 are even, since XRD just gives information about a sub-cell of the true superstructure. The indexing of both neutron diffraction and electron diffraction patterns made it necessary to consider the mentioned doubled supercell [14], which had also been proposed by Moriga *et al* [12].

The room-temperature high-resolution neutron diffraction data were refined taking as starting model for the tilting of the Ni coordination polyhedra that found and described in [14]. Instead of $P2_1/n$, the more symmetrical $C2/c$ space group was used to describe the structure, $Z = 8$. Table 1 lists the atomic coordinates and other relevant parameters after

Table 1. Structural parameters of $LaNiO_{2.5}$ refined from neutron diffraction data at 295 K. Space group $C2/c$, $Z = 8$. The unit-cell parameters slightly differ from those determined from XRD due to the inaccuracy of the neutron wavelength. $a = 7.8426(4)$ Å, $b = 7.7988(4)$ Å, $c = 7.4720(4)$ Å, $\beta = 93.859(4)^\circ$, $V = 455.97$ Å^3. Discrepancy factors: $R_p = 4.64$, $R_{wp} = 5.95$, $R_I = 6.30$, $\chi^2 = 4.88$.

Atom	Site	x	y	z	B (Å^2)	f_{occ}
La	8f	0.2483(7)	0.2601(6)	0.2510(6)	0.32(6)	1.0
Ni1	4a	0	0	0	0.14(9)	0.5
Ni2	4b	0	0.5	0	0.07(9)	0.5
O1	8f	0.2618(8)	0.0348(5)	0.0282(6)	0.46(9)	1.0
O2	8f	−0.0295(6)	0.2669(9)	0.0429(5)	0.65(9)	1.0
O3	4e	0	−0.054(1)	0.25	0.93(16)	0.5
O4	4e	0	0.49(1)	0.25	1.0	0.06(1)

the final refinement. A list of selected interatomic distances and angles can be found in table 2. The agreement between the observed and calculated neutron diffraction profiles is shown in figure 2.

Table 2. Selected distances (Å) and angles (°) for $LaNiO_{2.5}$.

LaO_7 polyhedra				
La–O1	2.428(6)			
–O1	2.709(6)			
–O1	2.626(7)			
–O2	2.591(7)			
–O2	2.383(7)			
–O2	2.707(7)			
–O3	2.446(7)			
–O4[a]	2.63(6)			
–O4[a]	2.91(7)			
NiO_6 octahedra				
Ni1–O1	2.068(6)	×2	O1–Ni1–O2	88.5(4)
–O2	2.121(7)	×2	O1–Ni1–O3	89.7(3)
–O3	1.916(2)	×2	O2–Ni1–O3	93.7(4)
NiO_4 square planes				
Ni2–O1	1.913(6)	×2	O1–Ni2–O2	89.2(4)
–O2	1.863(7)	×2		
–O4[a]	1.871(5)	×2		
			Ni1–O1–Ni2	160.1(2)
			Ni1–O2–Ni2	156.3(3)
			Ni1–O3–Ni2	154.21(8)

[a] O4 has a population factor of 0.06 atoms per formula.

Figure 3 shows a view of the crystal structure of $LaNiO_{2.5}$. It is a defect perovskite in which the oxygen vacancies are ordered in the *ab* plane along the [1 1 0] directions. The structure is constituted by NiO_6 octahedra (Ni1), sharing apical O3 oxygens along *c*. The octahedra share corners via O1 and O2 equatorial oxygens with NiO_4 square planar units

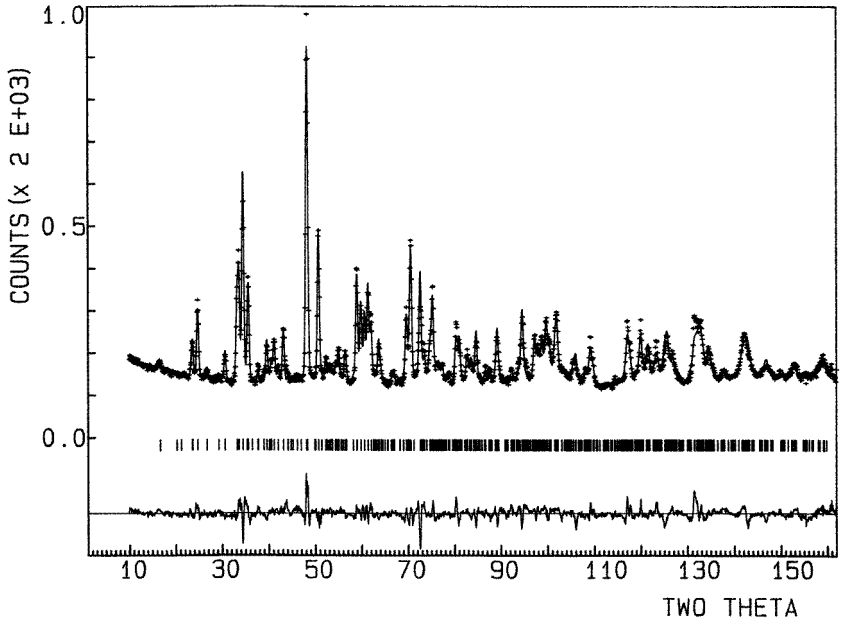

Figure 2. Observed (crosses), calculated (full line) and difference neutron diffraction profiles of $LaNiO_{2.5}$ at 295 K, collected in the high-resolution D2B diffractometer.

(Ni2), in such a way that NiO_6 and NiO_4 coordination polyhedra alternate along [1 0 0] and [0 1 0] directions. Both kinds of Ni polyhedron are rather tilted in order to optimize the La–O distances. The refinement of the occupancy factor of the residual oxygen atoms (O4) at the apical positions of the square planar units led to a small but significant value of 0.06(1) oxygen atoms per formula, distributed at random at $(0, 0.49(1), 1/4)$ positions. Thus, the crystallographic formula of this compound is $LaNiO_{2.56(1)}$. The presence of a slight oxygen excess has also been confirmed by thermal analysis, which gave a composition of $LaNiO_{2.53(1)}$.

NiO_6 octahedra are rather distorted, showing Ni–O bonding distances from 1.916(2) Å along the $\boldsymbol{c}$ axis, for Ni1–O3, to 2.121(7) Å, for N1–O2. NiO_4 square planes are slightly elongated along the $\boldsymbol{a}$ axis, with bondlengths of 1.863(7) Å (Ni2–O2) and 1.913(6) Å (Ni2–O1). The bonding distance from the residual O4 oxygens to Ni2 is 1.871(5) Å. La cations occupy a very irregular oxygen environment in sevenfold coordination, with La–O distances ranging from 2.383(7) to 2.709(6) Å.

3.2. Low-temperature neutron diffraction

The neutron diffraction patterns collected in the temperature range 1.5–250 K were also refined by the Rietveld method, taking as structural model that determined at room temperature. The observed and calculated profiles for the 1.5 K data are shown in figure 4. The observation of very weak additional reflections in the pattern below 80 K suggests the presence of long-range magnetic ordering. The new reflections (inset of figure 4) can be indexed in a cell with doubled a and b parameters, due to the antiferromagnetic ordering of the Ni moments. The most intense magnetic reflection is $(\frac{1}{2}, \frac{1}{2}, -1)$ (at $2\theta \approx 22.1^\circ$) as shown in figure 4. The proposed magnetic structure consists of antiferromagnetic chains of

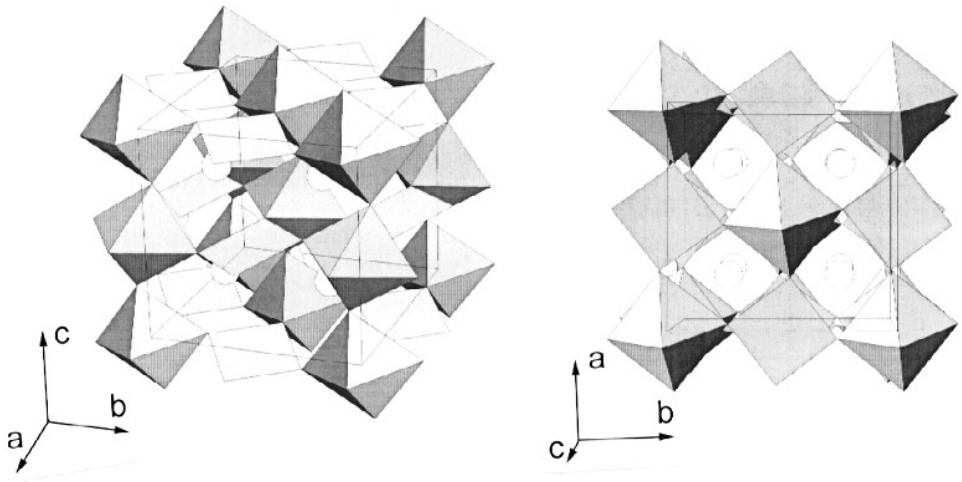

Figure 3. Two perspectives of the $LaNiO_{2.5}$ structure. NiO_6 octahedra and NiO_4 square planes alternate in the *ab* plane, in such a way that NiO_6 octahedra form chains along the *c* axis. La atoms (open circles) are in the voids formed by the Ni polyhedra.

NiO_6 octahedra parallel to the $\boldsymbol{c}$ axis. The experimental intensities are consistent with the absence of ordered moments at the square planar NiO_4 units, whereas any chain of NiO_6 octahedra is antiferromagnetically coupled to half of its four nearest-neighbour chains and ferromagnetically coupled to the other half (see figure 4). The best arrangement has been found for ordered moments with the following components: $m_x = 0.5(2)\ \mu_B$, $m_y = 0$, $m_z = 1.9(3)\ \mu_B$, for Ni cations at the octahedral positions. The corresponding experimental and calculated integrated intensities at 1.5 K are given in table 3 for the main magnetic reflections.

Table 3. Observed and calculated integrated magnetic intensities (in barns/unit cell) of $LaNiO_{2.5}$ at 1.5 K (according to the magnetic model described in the text).

h	k	l	I_{obs}	I_{calc}
$\frac{1}{2}$	$\frac{1}{2}$	-1	84	80
$\frac{1}{2}$	$\frac{1}{2}$	1	19	11
$\frac{1}{2}$	$\frac{3}{2}$	1	43	45
$\frac{3}{2}$	$\frac{3}{2}$	-1	30	59

4. Discussion

The crystal structure of $LaNiO_{2.5}$, containing an ordered arrangement of NiO_6 and NiO_4 polyhedra, is driven by the tendency of Ni^{2+} to adopt octahedral and square planar coordination, as already suggested by Rao *et al* [11]. Nevertheless, the structure contains several interesting features, concerning the tilting, size and distortion of the Ni coordination polyhedra that must be discussed. Firstly, the tilting of the Ni coordination polyhedra is considerably more severe than that observed in the precursor perovskite, $LaNiO_3$. The tilting can be quantified by the value of the Ni–O–Ni angles between two adjacent polyhedra.

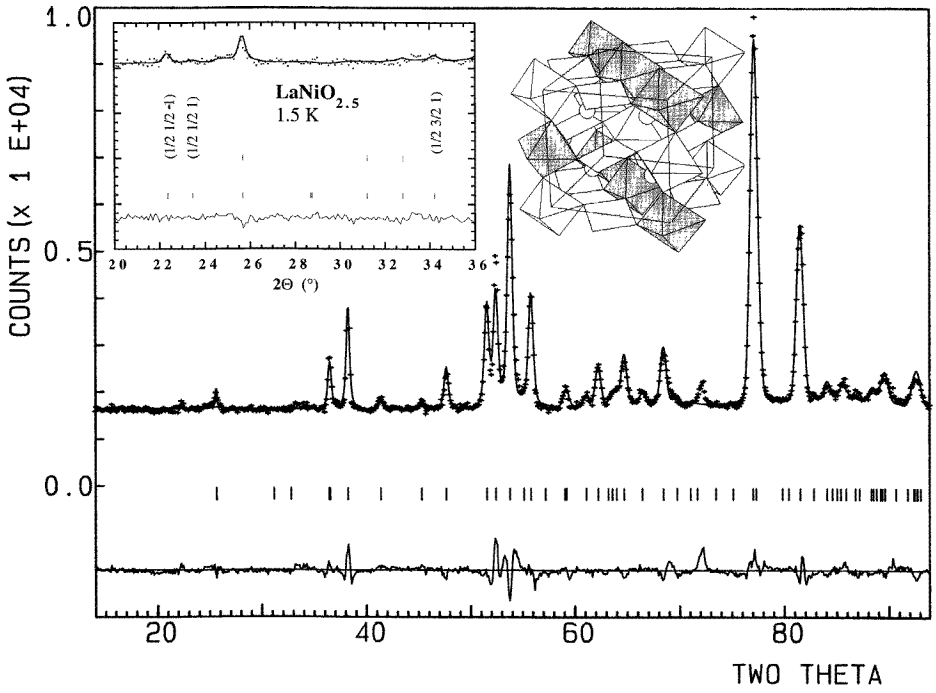

Figure 4. Profile refinement of the neutron diffraction data collected at 1.5 K in the G41 diffractometer. The inset in the small-angle region shows the fitting of the magnetic reflections. The two series of tick marks correspond to the allowed Bragg reflections for the crystal and magnetic structures, respectively. In the view of the structure, dark and white octahedra contain Ni^{2+} with magnetic moments parallel or antiparallel to the $\boldsymbol{c}$ axis.

Note that in $LaNiO_{2.5}$ these angles range from 154.2(8) to 160.1(2)°, whereas in $LaNiO_3$ the Ni–O–Ni angle [4] is 164.2(1)°, much closer to 180°. On the other hand, the kind of octahedral tilt, in Glazer's nomenclature [16], is $\boldsymbol{a}^-\boldsymbol{a}^-\boldsymbol{a}^-$ for $LaNiO_3$ (considering the pseudocubic rhombohedral axes), and can be defined as $\boldsymbol{a}^-\boldsymbol{a}^-\boldsymbol{c}^-$ for $LaNiO_{2.5}$. Note that the basic tilting scheme remains unchanged from the precursor to the defect perovskite; i.e. in both structures the polyhedra are tilted in antiphase along the three crystallographic axes, although in the latter the $\boldsymbol{c}$ axis is different (shorter) due to the presence of oxygen vacancies in the apical positions of alternating rows of octahedra. As suggested in [14], the observed shortening of the $\boldsymbol{c}$ axis must be attributed to the strengthening of the axial Ni1–O3 bonds rather than to the ordered absence of some oxygen atoms: the direct effect of these vacancies would rather be the expansion of the lattice along $\boldsymbol{c}$ due to the electrical repulsion between adjacent Ni cations.

The origin of the important structural stresses in the crystal can be better estimated through the calculation of the valence of the cations and anions present in the solid, by means of the Brown's bond valence model [17, 18]. This model gives a phenomenological relationship between the formal valence of a bond and the corresponding bond length. In perfect nonstrained structures the bond valence sum (BVS) rule states that the formal charge of the cation (anion) is equal to the sum of the bond valences around this cation (anion). This rule is satisfied only if the stress introduced by the coexistence of different structural units can be relieved by the existence of enough degrees of freedom in the crystallographic

structure. The departure from the BVS rule is, therefore, a measure of the existing stress in the bonds of the structure.

Table 4. Bond valences (s_i) for La–O and Ni–O bonds, multiplicity of the bonds (m) and valences ($\sum s_i$) for La and Ni cations within the respective coordination polyhedra in the $LaNiO_{2.5}$ structure. Bond valences are calculated as $s_i = \exp[(r_0 - r_i)/B]$; $B = 0.37$; r_0(La) = 2.172 Å, r_0(Ni) = 1.654 Å for the La^{III}–O^{2-} and Ni^{II}–O^{2-} pairs, respectively (from [18]). Individual La–O and Ni–O distances are taken from table 2. Bonds to O4 are not considered in the calculation.

Atom	s_i [m]				$\sum s_i$
La	0.501(9) [1]	0.235(4) [1]	0.293(5) [1]		
	0.323(6) [1]	0.57(1) [1]	0.236(4) [1]	0.48(1) [1]	2.63(1)
Ni1	0.327(5) [2]	0.283(5) [2]	0.492(3) [2]		2.20(1)
Ni2	0.497(8) [2]	0.57(1) [2]			2.13(2)

Table 4 lists the valences calculated for Ni and La from the individual Ni–O and La–O distances of table 2. Ni1 and Ni2 cations exhibit valences of +2.20(1) and +2.13(3), slightly higher than those expected in this compound, of +2. In compensation, the valence of the La cation is somewhat lower than +3. This result shows that Ni cations are overbonded while La atoms are underbonded in this structure; in other words Ni–O bonds are under compressive stress and La–O bonds are under tensile stress, giving rise to a structure with a relatively high metastable character. In fact, stresses can be relieved by hole doping of the structure: the compound readily takes oxygen, at temperatures over 175 °C in air, leading to the much more stable $LaNiO_3$ structure. In $LaNiO_3$ the bond-length values indicate the absence of tensile or compressive stresses: valences of +3.05 and +3.01 are obtained for La and Ni, respectively, from the La–O and Ni–O distances determined in a neutron diffraction study [4].

Moriga *et al* [12] proposed that $LaNiO_{2.5}$ contains octahedral Ni^{3+} and square planar Ni^{+} cations, from structural and magnetic considerations. This suggestion is in disagreement with the result of the present bond valence study, allowing us to check the valence of Ni within both octahedral and square planar coordination polyhedra. We can conclude that Ni cations are formally divalent in both oxygen environments. We are in the presence of a paradigmatic example, in the crystal chemistry of oxides, of a crystal structure with a transition metal showing the same oxidation state in ordered octahedral and square planar coordination polyhedra. Many examples exist, nevertheless, of structures in which a transition metal adopts octahedral and tetrahedral coordination polyhedra, for instance in the brownmillerite structure, typified by $CaFeO_{2.5}$ [19].

The magnetic properties of $LaNiO_{2.5+x}$ have been shown to be very dependent on the presence of small amounts of excess oxygen. An antiferromagnetic behaviour has been described for stoichiometric $LaNiO_{2.5}$ [12], whereas $LaNiO_{2.6}$ [13] was reported to exhibit ferromagnetism below $T_C \approx 230$ K. In our case, the magnetic behaviour of the defect perovskite phase was masked in the susceptibility curves by the presence of small amounts of Ni metal, undetected in XRD or NPD diagrams. However, low-temperature neutron diffraction experiments revealed the existence of long-range antiferromagnetic ordering below $T_N \approx 80$ K: very weak reflections of magnetic origin were observed in the NPD patterns below this temperature. The new reflections can be indexed with integer indices in a lattice with doubled $\boldsymbol{a}$ and $\boldsymbol{b}$ axes relative to the monoclinic crystal cell ($2\boldsymbol{a} \times 2\boldsymbol{b} \times \boldsymbol{c}$). Since the intensities of the reflections of magnetic origin are very small it is somewhat risky to draw conclusions concerning the exact magnetic arrangement of the moments in

the structure. Nevertheless, the model described in the results section for the magnetic structure reproduces satisfactorily the observed magnetic intensities. The magnetic structure contains antiferromagnetic chains of NiO_6 octahedra parallel to the $\boldsymbol{c}$ axis with an ordered moment at the NiO_6 octahedra ($m = 1.9(2)\ \mu_B$) which suggests the presence of high-spin Ni^{2+} cations ($S = 1$) at this site. The experimental intensities are also consistent with the absence of ordered moments at the square planar NiO_4 units, although the low intensity of the magnetic reflections make it difficult to establish a definitive conclusion.

The results concerning the low-temperature magnetic structure, suggesting the presence of Ni^{2+} cations in both coordination environments, with high-spin state ($S = 1$) at NiO_6 and low spin ($S = 0$) at NiO_4 polyhedra, are consistent with the results of the bond valence study from room-temperature structural data, and from the expected electronic configurations for Ni^{2+} in both coordination polyhedra. In an octahedral crystal field Ni^{2+} exhibits a $t_{2g}^6\ e_g^2$ configuration, with two unpaired electrons in the degenerate $d_{x^2-y^2}$ and d_{z^2} orbitals, with a high-spin ($S = 1$) state. In a square planar crystal field the degeneracy of the e_g orbitals is lost, and a low-spin ($S = 0$) configuration becomes the ground state. Nevertheless, the presence of some extra oxygen (0.06(1) atoms per formula) distributed at random in the axial positions of the square planar units should induce an slight increment in the average oxidation state of the Ni cations in planar coordination, thus slightly increasing the value of the magnetic moment of nickel in NiO_4. Therefore, the presence of a small moment associated with the square planar units should not be discarded.

5. Conclusions

The $LaNiO_{2.5}$ crystal structure shows a monoclinically distorted superstructure of perovskite of dimensions $2a_0 \times 2a_0 \times 2a_0$. It consists of infinite chains of flattened NiO_6 octahedra running along the $\boldsymbol{c}$ axis, connected in the ab plane by NiO_4 square planar units. The precise metal–oxygen distances derived from a neutron diffraction refinement of the structure allowed us to calculate the valences of Ni and La within their respective oxygen coordination polyhedra: this analysis clearly shows that Ni cations are divalent in both octahedral and square planar configurations. Below $T_N \approx 80$ K, a magnetic structure characterized by a propagation vector $\boldsymbol{k} = (\frac{1}{2}, \frac{1}{2}, 0)$ develops and accounts for the weak observed reflections of magnetic origin. This structure can be described as antiferromagnetic NiO_6 chains with $S = 1$ moments pointing along the chain direction ($\boldsymbol{c}$ axis). According to the proposed magnetic model, the moment at the NiO_4 units seems to be null or very small. The possibility of coexistence of low-spin Ni^{2+} ($S = 0$) at the square planar coordination and high-spin Ni^{2+} ($S = 1$) in octahedral coordination deserves further investigation.

Acknowledgments

The authors acknowledge the ILL and the LLB for making the neutron beam time available. They also thank the DIGCYT for financial support to the projects PB94-0046 and PB92-0849, and the EC HCM programme (contract No ERBCHGECT 920001).

References

[1] Lacorre P, Torrance J B, Pannetier J, Nazzal A I, Wang P W and Huang T C 1991 *J. Solid State Chem.* **91** 225
[2] Torrance J B, Lacorre P, Nazzal A I, Ansaldo E J and Niedermayer Ch 1992 *Phys. Rev.* B **45** 8209
[3] Goodenough J B and Raccah P 1965 *J. Appl. Phys.* **36** 1031

[4] García-Muñoz J L, Rodríguez-Carvajal J, Lacorre P and Torrance J B 1992 *Phys. Rev.* B **46** 4414
[5] Alonso J A, Martínez-Lope M J and Hidalgo M A 1995 *J. Solid State Chem.* **116** 146
[6] García-Muñoz J L, Suaaidi M, Martínez-Lope M J and Alonso J A 1995 *Phys. Rev.* B **52** 13 563
[7] Gai P L and Rao C N R 1975 *Z. Naturf.* a **30** 1092
[8] Crespin M, Levitz P and Gatineau L 1983 *J. Chem. Soc. Faraday Trans.* II **79** 1181
[9] Levitz P, Crespin M and Gatineau L 1983 *J. Chem. Soc. Faraday Trans.* II **79** 1195
[10] Vidyasagar K, Reller A, Golapakrishnan J and Rao C N R 1985 *J. Chem. Soc. Chem. Commun.* 7
[11] Rao C N R, Gopalakrishnan J, Vidysagar K, Ganguly A K, Ramanan A and Ganapathi L 1986 *J. Mater. Res.* **1** 280
[12] Moriga T, Usaka O, Imamura T, Nakabayashi I, Matsubara I, Kinouchi T, Kikkawa S and Kanamaru F 1994 *Bull. Chem. Soc. Japan.* **67** 687
[13] Moriga T, Usaka O, Nakabayashi I, Kinouchi T, Kikkawa S and Kanamaru F 1995 *Solid State Ion.* **79** 252
[14] Alonso J A and Martínez-Lope M J 1995 *J. Chem. Soc. Dalton Trans.* 2819
[15] Rodríguez-Carvajal J 1993 *Physica* B **192** 55
[16] Glazer A M 1972 *Acta Crystallogr.* B **28** 3384
[17] Brown I D 1981 *Structure and Bonding in Crystals* vol 2, ed M O'Keefe and A Navrotsky (New York: Academic) p 1
[18] Brese N E and O'Keefe M 1991 *Acta Crystallogr.* B **47** 192
[19] Beggren J 1971 *Acta Chem. Scand.* **25** 3616